Scar remodeling by Alginate Gel-Encapsulated Decoy Wnt receptor (sLRP6E1E2)-Expressing Adenovirus in a Pig Model

Sewoon Choi

Department of Medicine

The Graduate School, Yonsei University

Scar remodeling by Alginate Gel-Encapsulated Decoy Wnt receptor (sLRP6E1E2)-Expressing Adenovirus in a Pig Model

Sewoon Choi

Department of Medicine

The Graduate School, Yonsei University

Scar remodeling by Alginate Gel-Encapsulated Decoy Wnt receptor (sLRP6E1E2)-Expressing Adenovirus in a Pig Model

Directed by Professor Won Jai Lee

The Doctoral Dissertation
submitted to the Department of Medicine
the Graduate School of Yonsei University
in partial fulfillment of the requirements
for the degree of Doctor of Philosophy

Sewoon Choi

December 2019

This certifies that the Doctoral Dissertation of Sewoon Choi is approved.

Thesis Supervisor : Won Jai Lee

Thesis Committee Member#1 : Tai-Suk Roh

Thesis Committee Member#2 : Chae Ok Yun

Thesis Committee Member#3 : Ju Hee Lee

Thesis Committee Member#4 : Jae Jin Song

The Graduate School
Yonsei University

December 2019

ACKNOWLEDGEMENTS

I would like to express my deep gratitude to Dr. Tai- Suk Roh and Dr. Won Jai Lee for their valuable and constructive suggestions during planning and development of this research work.

I would also like to thank Dr. Ju Hee Lee, Pr. Chae Ok Yun and Pr. Jae Jin Song for their advise and assistance.

My grateful thanks are also extended to Dr. Jee Myung Kim of TL plastic surgery for enthusiastic encouragement and assistance in keeping my progress on schedule.

Finally I wish to thank my family for their support and encouragement through my study.

December 2019

Sewoon Choi.

<TABLE OF CONTENTS>

LIST OF FIGURES

ABSTRACT

Scar remodeling by Alginate Gel-Encapsulated Decoy Wnt receptor (sLRP6E1E2)-Expressing Adenovirus in a Pig Model

Sewoon Choi

Department of Medicine

The Graduate School, Yonsei University

(Directed by Professor Won Jai Lee)

An adenoviral vector (Ad) expressing a Wnt decoy receptor (sLRP6E1E2) is known to induce an anti-fibrotic effect by inhibiting Wnt signaling. We evaluated its effects in vivo using pig models and attempted to introduce an alginate gel-matrix system to prolong the effect of the Ad. Transduction efficiency was compared by fluorescent micrographs for the comparison of biological activity of Ad in different form; naked, gel-released and Ad in dissolved gel. And then, 50 days after the formation of full-thickness skin defects on the backs of Yorkshire pigs, scars were divided into five treatment groups: I, control, II, alginate gel, III, alginate gel capsulated control, IV, naked LRP6, and V, alginate gel capsulated LRP6. To evaluate its therapeutic efficacy, scar size and color index were compared, and various factors influencing scar formation and collagen rearrangement were analyzed through histology, immunohistochemistry and immunofluorescence assay. Real-time reverse transcriptase-polymerase chain reaction (RT-PCR) was also analyzed for evaluation of expression levels of TGF-β1, TGF-β3, MMP-1, TIMP1, and α-SMA mRNAs. And to examine inflammatory cell infiltration within the scar tissues, the number of inflammatory cells was calculated from four serial H&E-stained tissue sections.

GFP expression from gel-released Ad and Ad in dissolved gel was much higher than naked Ad. The size and color index of the scars has improved for the Ad treated group in pig model. The alginate gel encapsulating dE1-k35/sLRP6E1E2 treated scars (group V) were significantly improved in terms of scar surface size, erythema and melanin indices compared to other groups. Masson's trichrome stain showed that premature collagen deposition was markedly decreased in group V scar tissues compared to the other groups. Picrosirius red stain also revealed that sLRP6E1E2 induces collagen rearrangement to resemble that of mature, bundle-shaped collagen fibers, and gel encapsulation enhances its efficacy. Expression levels of the major ECM components; collagen I, elastin, and fibronectin, are significantly decreased by sLRP6E1E2 overexpression, especially in the alginate gel reservoir. And the alginate gel encapsulating dE1-k35/sLRP6E1E2-treated scar tissues (group V) showed decreased TGF-β1 mRNA expression and increased TGF-β3 mRNA expression compared with other groups. The treatment also increases matrix metalloproteinase-1 mRNA expression and decreases tissue inhibitor of metalloproteinases-1 and alpha-smooth muscle actin mRNA expression in pig scar tissues. And Alginate gel encapsulating dE1-k35/sLRP6E1E2 decreases inflammatory cell counts and mast cell counts in pig scar tissues.

Decoy Wnt receptor (sLRP6E1E2)-expressing adenovirus treatment improved scar quality in a pig model. Loading this construct in alginate gel allows sustained virus release into local tissues and prolongs Ad activity, thus maintaining its therapeutic effect longer in vivo. These advantages of the Ad/alginate system could markedly augment scar remodeling effects of sLRPE1E2 on scar tissue by steadily providing a high concentration of Ad with minimal toxicity.

---

key words : gene therapy, adenovirus, scar, alginate gel, decoy Wnt receptor, pig model

Scar remodeling by Alginate Gel-Encapsulated Decoy Wnt receptor (sLRP6E1E2)-Expressing Adenovirus in a Pig Model

Sewoon Choi

Department of Medicine

The Graduate School, Yonsei University

(Directed by Professor Won Jai Lee)

I. INTRODUCTION

Some wounds undergo abnormal healing process and leave disfiguring scars. Hypertrophic scars and keloids are representative examples of healed skin that is exceptionally red, thick, protruded, and tight. Various mechanisms have been proposed to explain keloid pathogenesis, but, treatment of keloids is extremely difficult as keloids frequently form at the site of injury, recur after excision, and always overgrow beyond the boundaries of original wound. These abnormal scarring is usually the result of unbalanced collagen production and degradation. Chronic, persistent, and prolonged proliferation of fibroblast leads to excessive synthesis and deposition of extracellular matrix (ECM) components, especially collagen. Although patients usually suffer from aesthetic disturbances and functional problems, these scars are difficult to

treat due to their complex pathophysiology and unknown polygenetic precipitating factors[1-3]. The response to treatment among patients is highly variable, and currently available therapies often achieve only temporary improvement.[1,4,5]

Transforming growth factor-β (TGF-β) is a key regulator of fibroblast activation that drives the excessive synthesis of ECM in fibrotic diseases. Recently, signaling cross-talk between the Wnt/β-catenin, TGF-β1, and Smads are demonstrated, where Wnt/β-catenin signaling activates TGF-β1 and TGF-β1 promotes Wnt/β-catenin signaling. Therefore, inhibition of the canonical Wnt pathway can be an effective approach to target TGF-β1 signaling which both can synergistically downregulate fibrogenesis. Therefore, on our previous research, we have demonstrated that soluble Wnt decoy receptor of LRP6 (sLRP6E1E2)-expressing Ad (dE1-k35/sLRP6E1E2), which expresses LRP6' E1 and E2 domain, prevents Wnt-mediated stabilization of cytoplasmic β-catenin and decreases Wnt/β-catenin signaling, and this construct can degrade extracellular matrix in HDFs, KFs, and primary keloid spheroids, and thus it may be beneficial for treatment of keloids[6].

Although adenoviral vectors are popular for gene therapy due to their high gene-transfer efficiency, they can deteriorate rapidly within a few weeks due to a short half-life, enzymatic inactivation, and transient effects. This may require repeated administration of an adenovirus to generate the desired anti-fibrotic effect, and regional administration of a high concentration of Ad can impair potential therapeutic effect and decrease safety. To deal with these problems, we loaded the virus in a sodium alginate-based hydrogel, which is a natural polymer frequently used in biomedical applications[7-9]. Alginate gel can be used as a depot system for the sustained release of Ad and maintaining Ad viral activity without affecting its biological activity[7,8]. Also, on previous researches, we examined that the use of alginate gel could increase therapeutic efficacy of adenovirus in a pig scar model[10].

In this study, we investigated the anti-fibrotic and scar remodeling effect of decoy Wnt receptor (sLRP6E1E2)-expressing adenovirus in vivo animal model. And we also demonstrate the use of an alginate gel-matrix system as a delivery vehicle to entrap sLRP6E1E2-expressing Ad for sustained release to promote scar tissue remodeling in a pig model.

II. MATERIAL AND METHODS

1. Preparation of Ad and alginate gel

A replication-incompetent Ad expressing the Wnt decoy receptor (dE1-k35/sLRP6E1E2) and control Ad (dE1-k35/LacZ)[11] were used in this study. The propagation, purification, and titration of Ad were performed as previously described[12,13] . An alginate (alginic acid sodium salt, Sigma, St. Louis, MO) solution of 5 wt% was prepared with 0.5 g alginate and 0.09 g NaCl (Sigma) in 10 ml phosphate-buffered saline (PBS). The alginate solution was stirred for 24 h at room temperature and gelated in 50 mM $CaCl_2$ (Sigma)[7].

2. Biological activity of encapsulated Ad

To compare the biological activity of Ad in different forms, Ad (1×10^{10} VP of dE1/GFP) was encapsulated in 5% alginate gel, and incubated with Dulbecco's modified Eagle's medium at 37°C for 1, 3, 5, 7, 9 and 11 days. At each time point, medium that containing the released Ad was collected (gel-released Ad), and the remaining Ad/alginate gel was dissolved (Ad in dissolved gel). SK-Hep 1 cells were then transduced with naked Ad, gel-released Ad, and Ad in dissolved gel. Transduction efficiency was compared in fluorescent micrographs showing SK-Hep1 cells incubated with Ad in each form.

3. Scar formation

Female Yorkshire pigs (4 months of age, 40 kg) were used for the scar model. This animal study was approved by an institutional review board of Yonsei university. All animal experimental procedures were performed in accordance with the relevant guidelines and regulations of the Department of Laboratory Animal Resources, Yonsei Biomedical Research Institute, Yonsei University College of Medicine. Anesthesia was induced in each pig via intramuscular injection of Zoletil® (5 mg/kg, Virbac, Carros, France) and Rompun® (2 mg/kg, Bayer, Seoul, Korea) and maintained through inhalation of isoflurane (IsoFlo®, Abbott Laboratories, Abbott Park, Illinois). After complete hair removal, 36 full-thickness skin defects ($3\times3cm^2$) were created symmetrically on the back of each Yorkshire pig, with 18 wounds on each side of the midline. The wound was spaced at least 3cm apart and reached the depth of the muscle fascia to mimic human scar formation. Intravenous antibiotics were administered, and TegaDerm® (3M, St Paul, MN) was used as wound dressing for 5 days. Scar tissues, which were distinct in appearance compared to the peripheral normal tissues, were formed 50 days after creating the initial skin defects.

4. Injection of Ad

Wound epithelialization and scar formation occurred on postoperative day 50. Scars were divided into five treatment groups: I, PBS (control, n=7); II, alginate gel (gel, n=7); III, alginate gel encapsulating dE1-k35/LacZ (gel+dE1-k35/LacZ, capsulated control, n=7); IV, naked dE1-k35/sLRP6E1E2 (naked LRP6, n=7); and V, alginate gel encapsulating naked dE1-k35/sLRP6E1E2 (gel+dE1-k35/sLRP6E1E2, capsulated LRP6, n=8) (5×10^7 PFU). Under anesthesia, viruses were injected with a 27-gauge needle with 1-ml syringe, and Ad/alginate gel mixtures were directly injected into the intradermal layers of the scar regions.

5. Therapeutic evaluation of scar size and erythema and melanin indices

The surface areas of the scars were imaged with a digital camera. The images were measured with a ruler and compared to a 1 cm^2 standard, and measurements were assessed with ImageJ software (National Institutes of Health, Bethesda, MD, USA). Scar color was quantitatively analyzed with a spectrophotometer (CM-700D; KONICA MINOLTA, INC., Tokyo, Japan). The color of each scar was examined with erythema (the degree of scar redness) and melanin (the degree of scar darkness) indices[14]. Each value was measured at least three times, and the mean was calculated. All of the evaluations were performed every 10 days until the 50th day after virus injection. We normalized the values of alginate gel (gel), alginate gel encapsulating dE1-k35/LacZ (capsulated control), naked dE1-k35/sLRP6E1E2 (naked LRP6), and alginate gel encapsulating dE1-k35/sLRP6E1E2 (capsulated LRP6)-treated scars to that of PBS-treated scars.

6. Histology and immunohistochemistry

Representative sections were stained with hematoxylin & eosin (H&E) and Masson's trichrome before examination under light microscopy. Scar tissue sections were incubated at 4°C overnight with one of the following primary antibodies: mouse anti-collagen type-I (ab6308; Abcam, Ltd., Cambridge, UK), mouse anti-elastin (E4013; Sigma-Aldrich Co.), and mouse anti-fibronectin (sc-52331; Santa Cruz Biotechnology, Santa Cruz, USA). Then, tissues were incubated at room temperature for 20 minutes with the DAKO Envision™ Kit (DAKO, Glostrup, Denmark) as a secondary antibody. Diaminobenzidine/hydrogen peroxidase (DAKO) was used as the chromogen substrate. All sections were counterstained with Meyer's hematoxylin. Expression levels of type I collagens, elastin, and fibronectin were semi-quantitatively analyzed with MetaMorph® image analysis software (Molecular Devices, Sunnyvale, CA, USA). Values are calculated as the mean optical density of six different digital images. Immunohistochemistry was performed by the same individual who was

blinded to the experimental group, and the tissue sections for analysis were obtained from the center areas of scar tissue.

Picrosirius red (Sigma-Aldrich Co.) staining was performed on specimens collected 5 or 50 days after experiments for evaluation of collagen-fiber arrangement with optical microscopy (BX51, Olympus, Tokyo, Japan) at ×200 magnification.

7. Immunofluorescence assay

Specimens were collected 5 and 50 days after treatment and were embedded in paraffin blocks. Paraffin-embedded tissues were sectioned, deparaffinized, rehydrated, and treated with blocking buffer (5% normal goat serum, S-100, Vector Laboratories Inc., Burlingame, CA, USA) for 1 hour. After removing the blocking buffer, sections were immersed in primary antibody (anti-Flag, Sigma) overnight at 4°C and then incubated in secondary antibody (rabbit anti-mouse FITC, Santa Cruz Biotechnology) at room temperature for 2 hours. Anti-Flag antibody was used to confirm the Flag-tagged LRP6. Confocal microscopy (LSM700, Carl Zeiss, Oberkochen, Germany) was performed on tissues were mounted on slides using Vectashield® mounting medium containing the nuclear stain DAPI (Vector Laboratories).

8. Real-time reverse transcriptase-polymerase chain reaction (RT-PCR) for expression levels of TGF-β1, TGF-β3, MMP-1, TIMP1, and α-SMA mRNAs

At 50 days after Ad injection, total RNA was prepared from tissue with TRIzol® reagent (Invitrogen, Carlsbad, CA, USA), and complementary DNA was prepared from 500 ng total RNA by Oligo dT (Bioneer Corp., Alameda, CA, USA) and a cDNA synthesis kit (Bioneer Corp.), under the following conditions: 42°C for 60 min, 94°C 5 min. Real-time PCR was performed with an StepOnePlus™ Real-Time PCR System (Thermo Fisher Scientific,

Waltham, MA, USA) and following a Taqman® Real-time PCR assay (Thermo Fisher Scientific) [assay ID: Ss03382325_u1 (TGF-β1), Ss03394349_g1 (TGF-β3), Ss04245657_g1 (matrix metalloproteinase-1, MMP-1), Ss03381944_u1 (tissue inhibitor of metalloproteinase 1, TIMP-1), and Ss04245588_m1 (α-smooth muscle actin, α-SMA)]. Target mRNA expression levels were normalized to that of β-actin (Thermo Fisher Scientific) [assay ID: Ss03376563_uH] levels, and relative quantization was expressed as fold-induction compared with control conditions in each tissue. PCR was performed three times for each mRNA in each tissue, and the average value was calculated.

9. Statistics

Results are expressed as the mean ± standard deviation (SD). Data were analyzed with repeated-measures one-way analysis of variance (ANOVA). Two sets of independent sample data were compared using paired t-tests; $p<0.05$ was considered statistically significant.

III. RESULTS

1. Ad is continuously released from the alginate gel, and gel encapsulation prolongs Ad biological activity

Transduction efficiency was compared by fluorescent micrographs showing SK-Hep1 cells incubated with Ad in different forms (Figure 1). GFP expression of naked Ad was noticeably decreased from the 3rd day of incubation and almost absent after the 7th day (Figure 1 upper low), whereas cells transduced with 5% gel-released Ad showed relatively strong and sustained GFP expression until the 11th day (Figure 1 middle low). Also, GFP expression of Ad in dissolved gel was prolonged and much higher than naked Ad (Figure 1 lower low). These results demonstrate that the alginate gel provides a biocompatible environment for Ad to maintain its viral activity and release Ad in sustained manner.

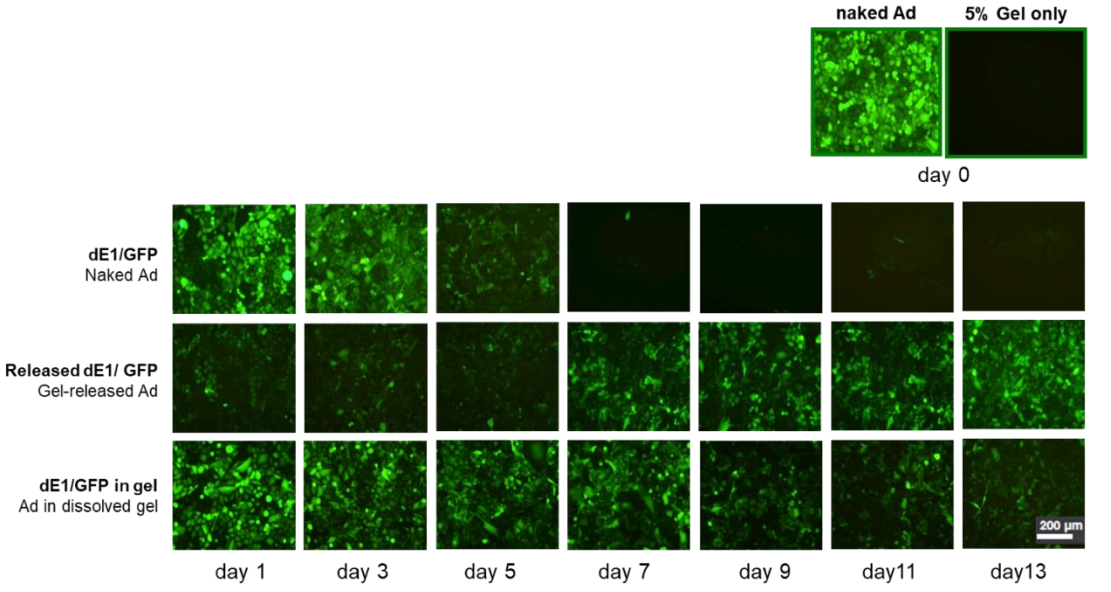

Figure 1. Comparisons of GFP expression level in each group. Fluorescent microscopies showing SK-Hep1 cells incubated with Ad in various forms. Ad (1x1010 VP of dE1/GFP) was encapsulated in 5% alginate gel, and incubated with Dulbecco's modified Eagle's medium at 37℃ for 1, 3, 5, 7, 9, 11, and 13 days. SK-Hep1 cells transduced with dE1/GFP (naked Ad, top row), released Ad from 5% gel (middle row), and dissolved Ad-gel (lower row). GFP expression from gel-released Ad and Ad in dissolved gel was much higher than naked Ad, demonstrates that the alginate gel provides a biocompatible environment for sustained release of Ad and maintenance of Ad viral activity.

We also examined sLRP6E1E2 expression by immunofluorescence staining of pig scar tissues. The alginate gel encapsulating dE1-k35/sLRP6E1E2 treated group (group V) showed markedly increased immune reactivity for sLRP6E1E2 compared to the other groups,

especially group IV 5 days after injection (Figure 2(a)), and persistent sLRP6E1E2 expression was observed 50 days after injection (Figure 2(b)). More importantly, the total level of sLRP6E1E2 expression from alginate gel encapsulating dE1-k35/ sLRP6E1E2 was much higher than naked dE1-k35/sLRP6E1E2 both 5 and 50 days after injection. This shows the potential utility of alginate gel encapsulating dE1-k35/sLRP6E1E2 for in vivo applications that require long-term and efficient gene transfer.

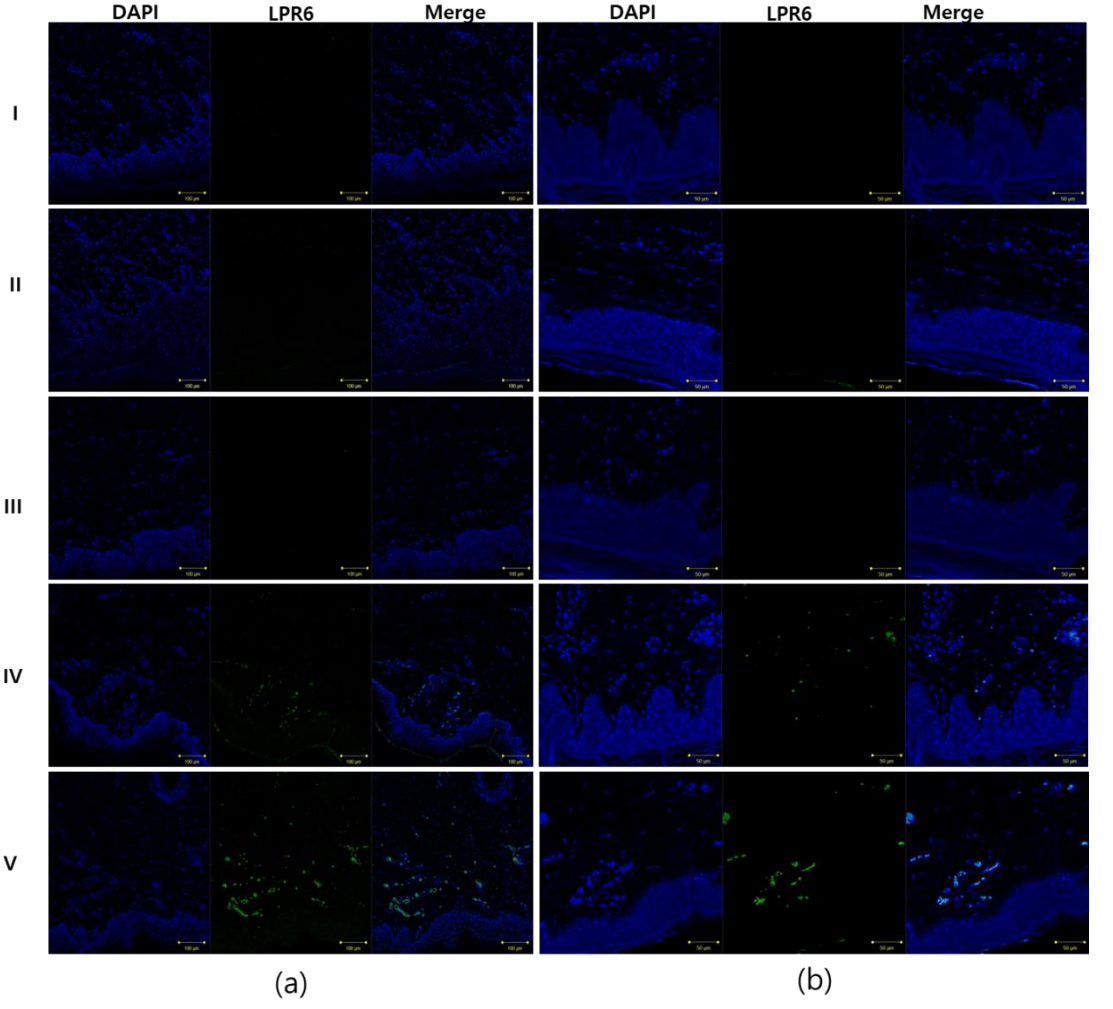

Figure 2. Immunofluorescence staining of pig scar tissues. (a) 200x. sLRP6E1E2 expression by immunofluorescence staining in pig scar tissues, 5th day after injection. The alginate gel encapsulating dE1-k35/sLRP6E1E2 treated group (Group V) showed markedly increased immune-reactivity.; (b)200x. sLRP6E1E2 expression by immunofluorescence staining in pig scar tissues, 50 days after injection. Group V showed persistent sLRP6E1E2 expression. The total level of sLRP6E1E2 expression from Group V was much higher than group IV, indicating the potential utility of gel encapsulation for long-term and efficient gene transfer.

2. sLRP6E1E2-expressing Ad/gel decreases scar size and color in pig scar tissue.

The therapeutic effect of sLRP6E1E2-expressing Ad on scar tissue was evaluated with scar size and erythema and melanin indices (Figure 3 and 4). The values listed below correspond to the following treatment groups: I, PBS (control); II, alginate gel (gel); III, alginate gel encapsulating dE1-k35/LacZ (gel+dE1-k35/LacZ; capsulated control); IV, naked dE1-k35/sLRP6E1E2 (naked LRP6); and V, alginate gel encapsulating naked dE1-k35/sLRP6E1E2 (gel+dE1-k35/sLRP6E1E2, capsulated LRP6). On the photographic evaluation on initial and 50 days after treatments, the scar areas decreased, and the color improved at 50 days after the injection of alginate gel encapsulating naked dE1-k35/sLRP6E1E2 (Group V) (Figure 3). Photographs of scars were taken before and after each treatment were taken and measured with Image J software.

The sizes of initial scars were measured as 1.46 ± 0.88 cm^2, 1.51 ± 0.79 cm^2, 1.21 ± 0.15 cm^2, 1.15 ± 0.18 cm^2, and 1.42 ± 0.3 cm^2 in each group, respectively, and there were statistically no differences. However, the sizes of the scars decreased to 1.14 ± 0.48 cm^2 (78% of initial scar, $p<0.05$), 0.81 ± 0.08 cm^2 (78% of initial scar, $p<0.05$), 0.96 ± 0.11 cm^2 (79% of initial scar, $p<0.05$), 0.81 ± 0.17 cm^2 (70% of initial scar, $p<0.05$), and 0.87 ± 0.19 cm^2 (61% of initial scar, $p<0.01$), respectively, by the 50th day after treatments, indicating that sLRP6E1E2

expression from Ad (groups IV and V) reduces scar size. Furthermore, alginate gel encapsulating dE1-k35/sLRP6E1E2 treated scars (group V) were only significantly reduced compared to control or scars treated with capsulated control virus ($p<0.05$, Figure 3 & 4, left).

The erythema indices of the initial scars were 2.9 ± 0.54, 3.12 ± 0.91, 2.77 ± 0.5, 2.32 ± 0.19, and 3.02 ± 0.48 in each group, respectively. Erythema was significantly decreased to 2.76 ± 0.55, 2.29 ± 0.43, 2.15 ± 0.32, 1.99 ± 0.39, and 1.88 ± 0.12 in each group, respectively, by the 50^{th} day after treatments. Compared to baseline, the ratio of erythema indices at 50 days treated with PBS, gel, capsulated control, naked LRP6, and capsulated LRP6 were 92%, 88%, 66%, 80%, and 59% ($p<0.01$) in each group, respectively. The alginate gel encapsulating dE1-k35/sLRP6E1E2 treated scars (group V) were significantly improved in terms of erythema compared to other groups ($p<0.05$; Figure 4, middle). Similarly, the melanin indices at 50 days were significantly reduced by 75%, 54%, 60%, 70%, and 5% ($p<0.01$) in each groups, respectively, showing that sLRP6E1E2 expression from gel-encapsulated Ad (group V) reduces the melanin indices of scars ($p<0.05$ vs. groups I to IV; Figure 4, right). Taken together, these results indicate that sLRP6E1E2-expressing Ad plays a prominent role in reducing scar size, erythema, and pigmentation. Notably, Ad in an alginate gel-matrix system showed more effective biologic activities than naked Ad.

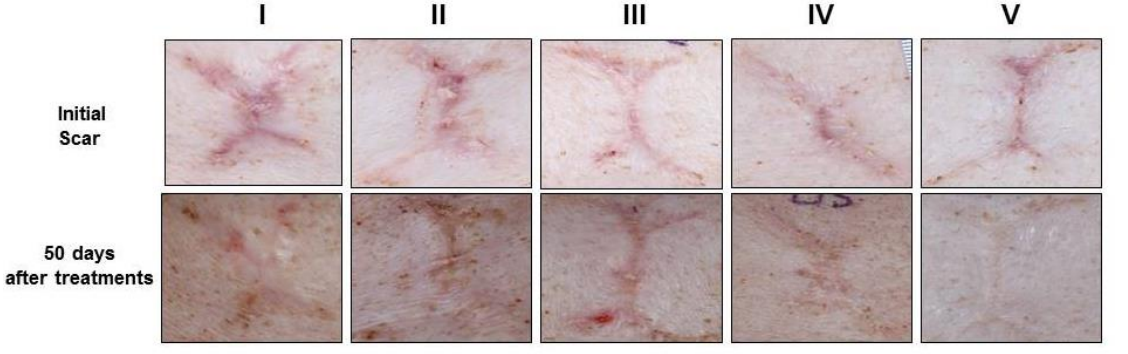

Figure 3. Photographic analysis of scar tissues. The photographs of scars before and 50 days after treatment in pigs of each group (Groups: I, PBS (control); II, alginate gel (gel); III, alginate gel encapsulating dE1-k35/LacZ (gel+dE1-k35/LacZ; capsulated control); IV, naked dE1-k35/sLRP6E1E2 (naked LRP6); and V, alginate gel encapsulating naked dE1-k35/sLRP6E1E2 (gel+dE1-k35/sLRP6E1E2, capsulated LRP6).

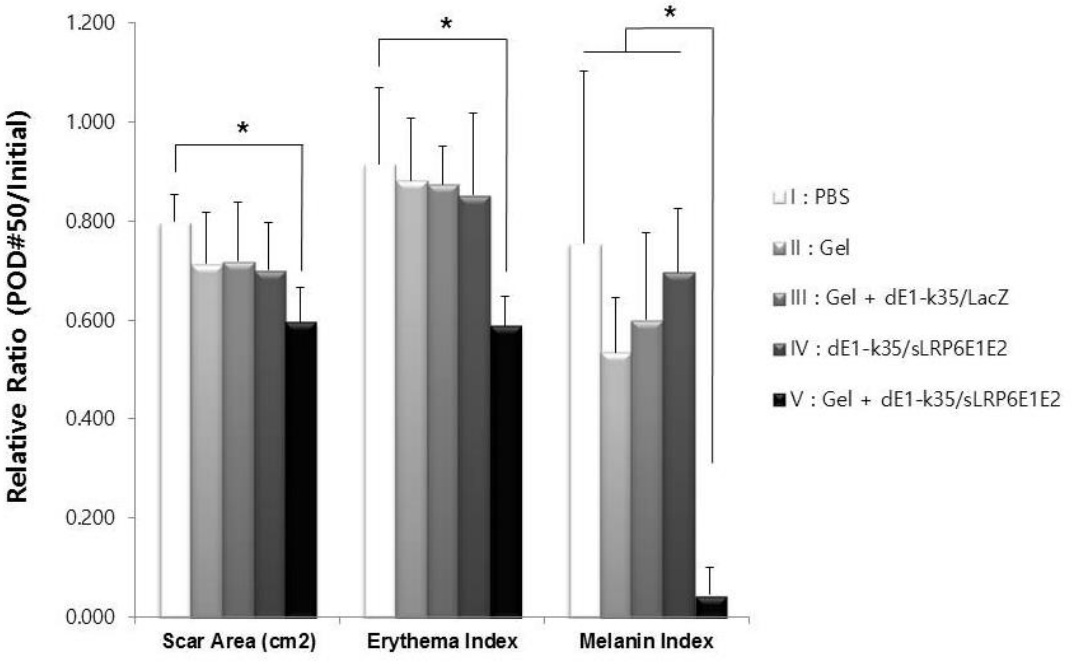

Figure 4. Therapeutic evaluation of scar area, color index, and pliability with Image J software and spectrophotometry. Therapeutic evaluation of the scars sLRP6E1E2-expressing Ad plays a prominent role in reduction of scar surface area and color (mainly composed of erythema and melanin). Ad with alginate gel-matrix system showed more effective biologic activities than naked Ad. Data are expressed as a mean±standard error of the mean.

3. sLRP6E1E2-expressing Ad/gel induces collagen rearrangement

Masson's trichrome stain was performed to evaluate the effects of sLRP6E1E2-expressing Ad on collagen-fiber arrangement. From the 5th day after treatments, premature collagens were deposited on scar tissues, but in group V, premature collagen deposition area was smaller than other groups (Figure 5a). However, on the 50th day after treatment, Masson's trichrome stain revealed that premature collagen deposition was markedly decreased in group V scar tissues (alginate gel encapsulating dE1-k35/sLRP6E1E2) compared to the other groups (Figure 5b).

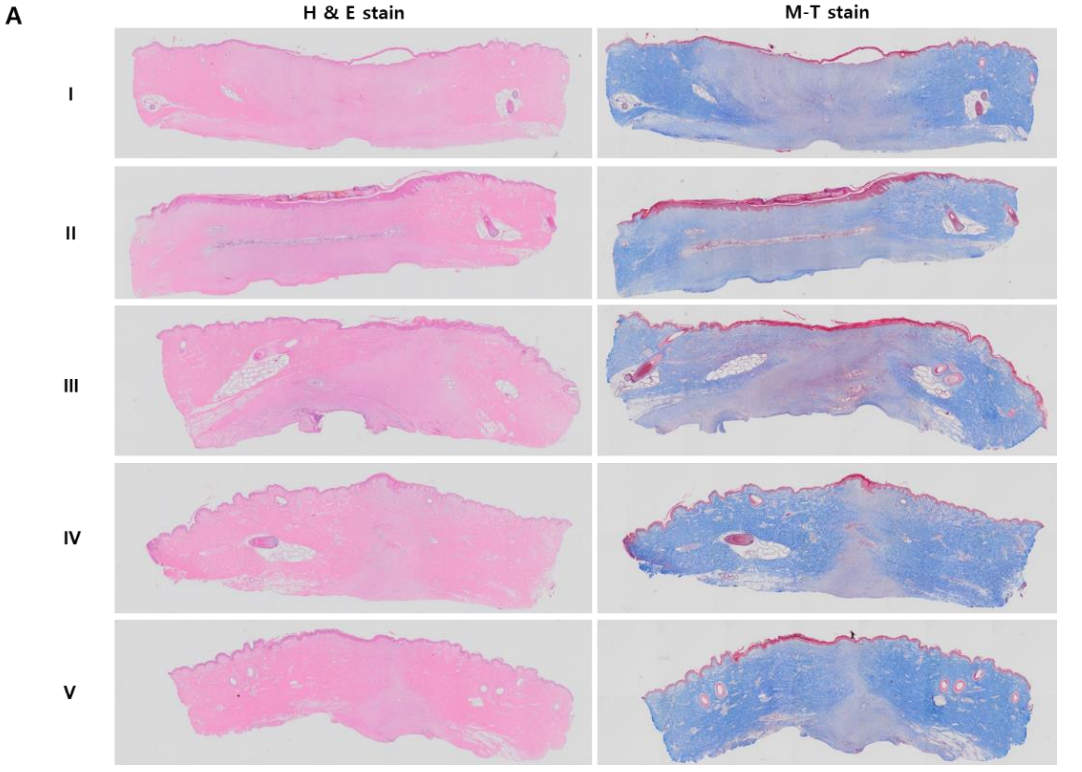

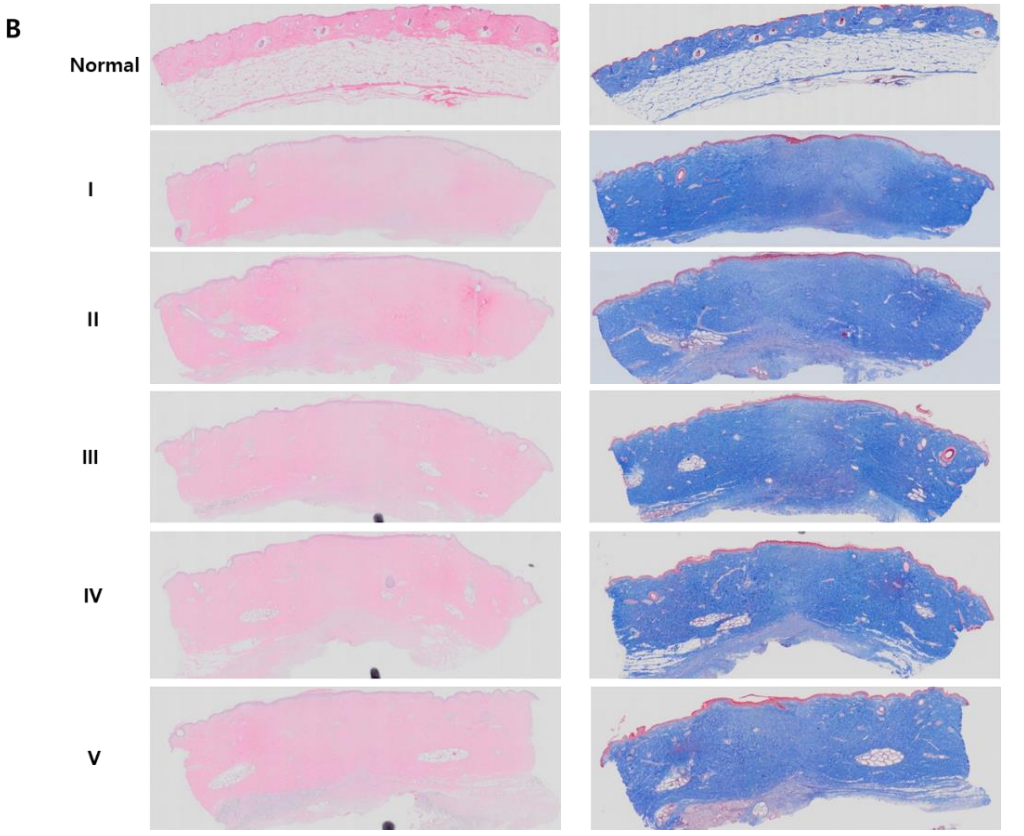

Figure 5. sLRP6E1E2-expressing Ad/gel induces collagen rearrangement. Masson's trichrome stain was performed to evaluate the effects of sLRP6E1E2-expressing Ad on collagen-fiber arrangement on the 5th (a) and 50th day (b) after treatments. Premature collagen deposition was markedly decreased in group V scar tissues (alginate gel encapsulating dE1-k35/sLRP6E1E2) compared to the other groups. original magnification, ×12.

Tissues were also stained with picrosirius red, which specifically binds collagen fibrils of various diameters. On the 50th day after treatment, premature collagen depositions were displaced by mature and well-arranged collagen bundles, and dense and coarse collagen bundles structure were replaced by thin and shallow collagen bundles. Furthermore, scar

tissues in groups IV and V had closely packed collagen fibers and formed complete bundles compared to other groups (groups I to III), which is similar to normal dermal structure (Figure 6). These data suggested that sLRP6E1E2 induces collagen rearrangement to resemble that of mature, bundle-shaped collagen fibers, and gel encapsulation enhances its efficacy.

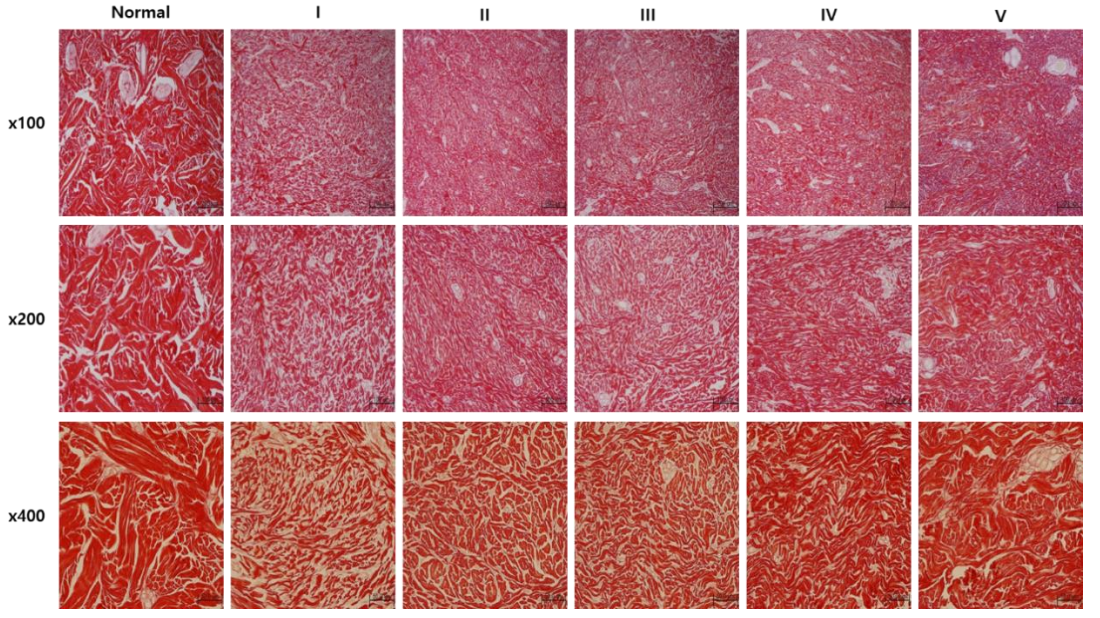

Figure 6. Picrosirius red staining in a pig scar tissues. On the 50th day after treatment, premature collagen depositions were displaced by mature and well-arranged collagen bundles, and scar tissues in groups IV and V had closely packed collagen fibers and formed complete bundles compared to other groups (groups I to III), which is similar to normal dermal structure.

4. sLRP6E1E2-expressing Ad/gel reduces collagen I, elastin, and fibronectin

We examined the effects of sLRP6E1E2 overexpression on the major ECM components of scar tissues. Immunohistochemical staining of scar sections revealed significant reductions in type I collagen and fibronectin in the alginate gel encapsulating dE1-k35/sLRP6E1E2-treated

group (group V) compared with other groups (**p<0.01, Figure 7). Reductions of elastin in naked dE1-k35/sLRP6E1E2-treated scar tissues (group IV) were significant compared to scars in groups I, II, and III, but smaller than that of group V. Taken together, these data strongly suggest that expression levels of the major ECM components are significantly decreased by sLRP6E1E2 overexpression, especially in the alginate gel reservoir.

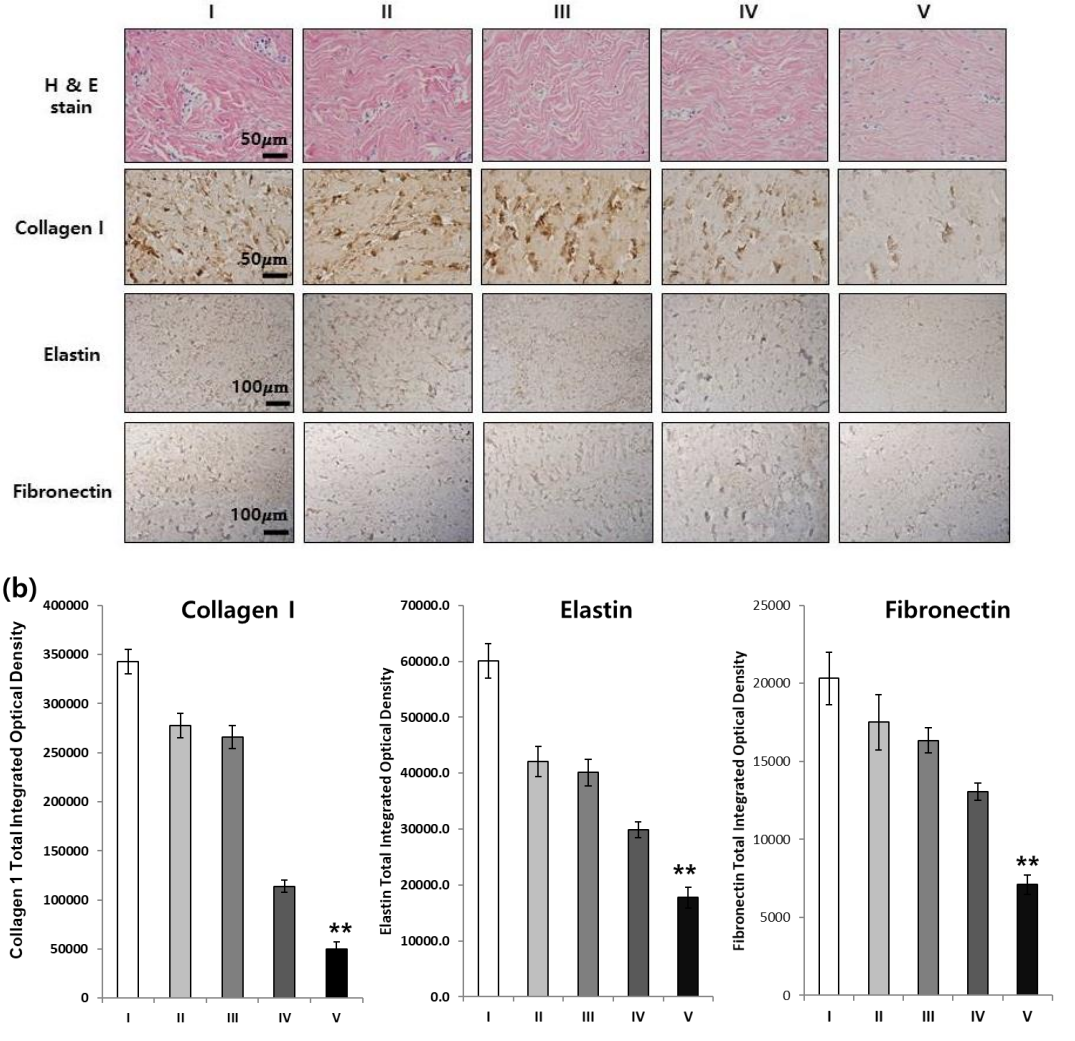

Figure 7. Immunohistochemical staining for collagen type-I, elastin, and fibronectin in pig scar tissues at 50th day after treatment (a) and semi-quantitative images analysis with MetaMorph® (b). The expression levels of the major extracellular matrix components type-I collagen, elastin, and fibronectin were lower in scar tissues treated with the alginate gel encapsulating group V compared with other groups, especially compared with group IV. (H&E, X 400, others, X200)

5. Alginate gel encapsulating dE1-k35/sLRP6E1E2 downregulates TGF-β1 and upregulates TGF-β3 mRNA expression in pig scar tissues

To examine the mechanism by which sLRP6E1E2-expressing Ad suppresses expression of the major ECM components in pig scar tissues, the change of TGF-β1 and TGF-β3 mRNA levels were evaluated on various groups by qRT-PCR. The alginate gel encapsulating dE1-k35/sLRP6E1E2-treated scar tissues (group V) showed decreased TGF-β1 mRNA expression and increased TGF-β3 mRNA expression compared with other groups (Figure 8). The TGF-β1 mRNA level of scar tissues from group V (Figure 8a) were 5- and 3-fold lower than that of groups I and IV, respectively (both $^{**}p < 0.001$). In addition, TGF-β3 mRNA levels of group V (Figure 8b) were 1.6-fold higher compared to group I and 1.8-fold higher compared to group IV (both $p < 0.001$). These results suggest that the reduced expression of ECM components by sLRP6E1E2 overexpression is associated with decreased TGF-β1 expression and increased TGF-β3 expression.

Scar remodeling-associated molecules such as MMP-1, TIMP-1, and α-SMA are important markers of the effects of TGF-β on wound repair. Therefore, we performed qRT-PCR analysis of MMP-1, TIMP-1, and α-SMA and showed differential expression of these matrix remodeling-associated molecules among experimental groups. MMP-1 expression levels of

group V scar tissues were significantly increased by 4.9- and 1.7-fold, respectively, versus those of groups I and IV scar tissues (both $p<0.001$, Figure 9(a)). In contrast, TIMP-1 and α-SMA expression levels of group V scar tissues were significantly decreased by 2.2- and 2.8-fold, respectively, compared to groups I and II (both $p<0.01$, Figure 9(b,c)). However, there was no significant difference between groups IV and V. These results suggest that sLRP6E1E2 upregulates MMP-1 and downregulates TIMP-1 and α-SMA, which are major players in collagen breakdown.

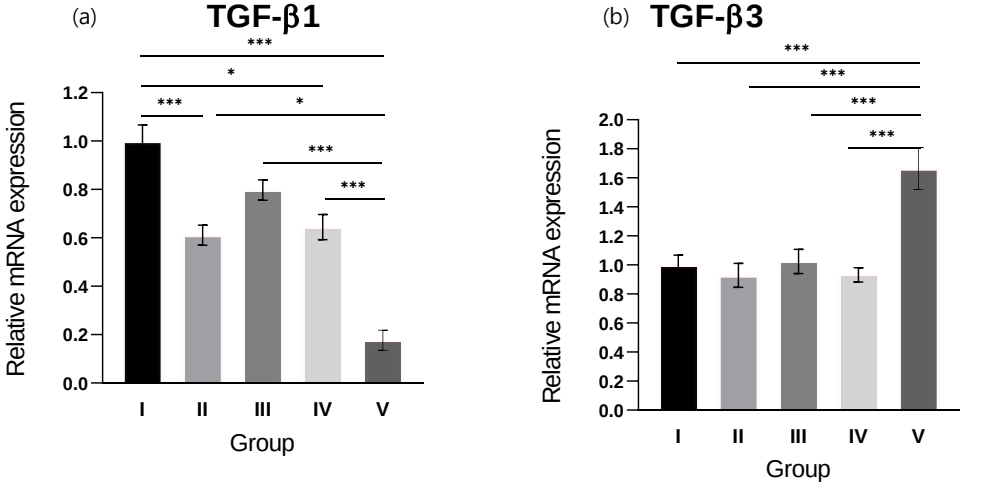

Figure 8. Alginate gel encapsulating dE1-k35/sLRP6E1E2 downregulates TGF-β1 and upregulates TGF-β3 mRNA expression in pig scar tissues. (a) TGF-β1 mRNA levels of group V were 5-fold lower than that of group I and 3-fold lower than that of group IV scar tissues. (b) TGF-β3 mRNA levels of group V were 1.6-fold higher than that of group I scar tissues and 1.8-fold higher than that of group IV scar tissues.

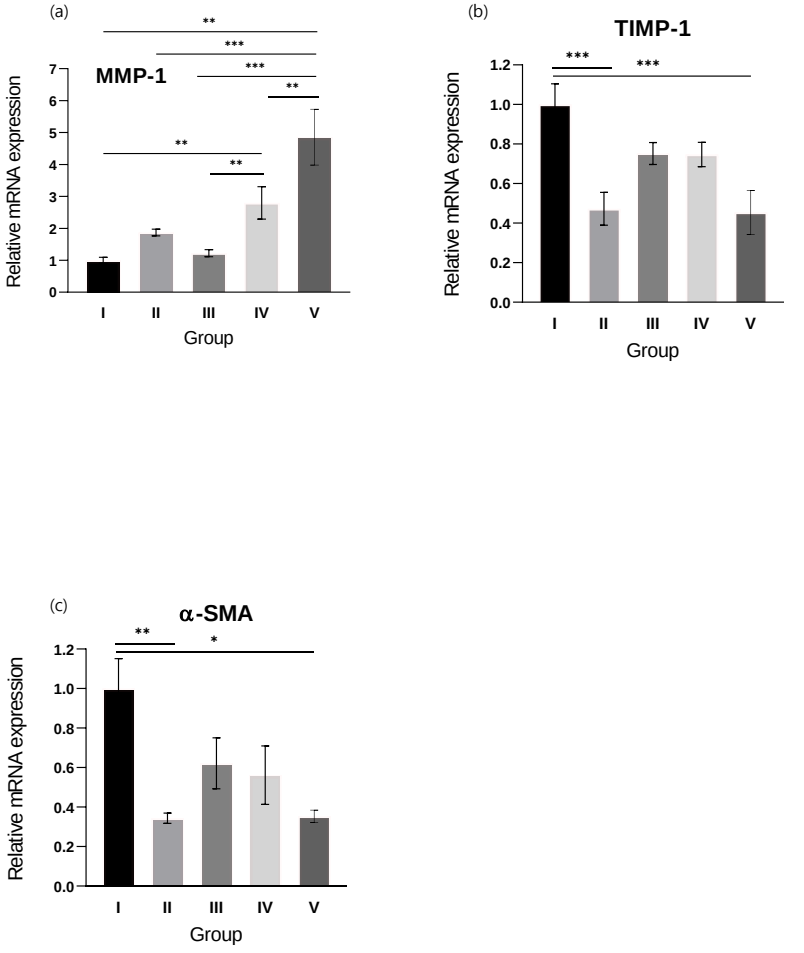

Figure 9. Alginate gel encapsulating dE1-k35/sLRP6E1E2 increases MMP-1 mRNA expression and decreases TIMP-1 and α-SMA mRNA expression in pig scar tissues (a) MMP-1 expression levels of group V scar tissues were significantly increased by 4.9- and 1.7-fold versus groups I and IV scar tissues, respectively (***p<0.001). In contrast, TIMP-1(b) and α-SMA expression(c) levels of group V scar tissues were significantly decreased by 2.2- and 2.8-fold versus group I scar tissues, respectively (*p <0.05, ** p <0.01, ***p < 0.001).

6. Alginate gel encapsulating dE1-k35/sLRP6E1E2 decreases inflammatory cell counts and mast cell counts in pig scar tissues

To examine inflammatory cell infiltration within the scar tissues, the number of inflammatory cells was calculated from four serial H&E-stained tissue sections. On day 5 of the postoperative period, the mean numbers of inflammatory cells within the scar tissue were 9.2±2.39, 9.25±2.63, 5.80±1.79, 7.75±1.71, and 2.20±1.30 in each groups, respectively. On day 50 of the postoperative period, these were 9±2.6, 8.5±1.41, 8±1.01, 6.28±0.84, and 3.35±0.30 in each groups, respectively. The numbers of inflammatory cells on Days 5 and 50 were significantly lower in the alginate gel encapsulating dE1-k35/sLRP6E1E2-treated scar tissues (group V) (* $p < 0.05$).

Mast cells are reported to be involved in the proliferation and contraction of fibroblasts, and the synthesis of ECM. They also play a key role in scar formation. On day 50 of the postoperative period, the mean numbers of mast cells were 10.17±0.6, 8.97±0.39, 8.53±0.52, 7.03±0.38, and 2.51±0.25 in each groups, respectively. A statistically significant decrease was seen in the mean number of mast cells in the alginate gel encapsulating dE1-k35/sLRP6E1E2-treated scar tissues (group V) in comparison of other groups (* $p < 0.05$).

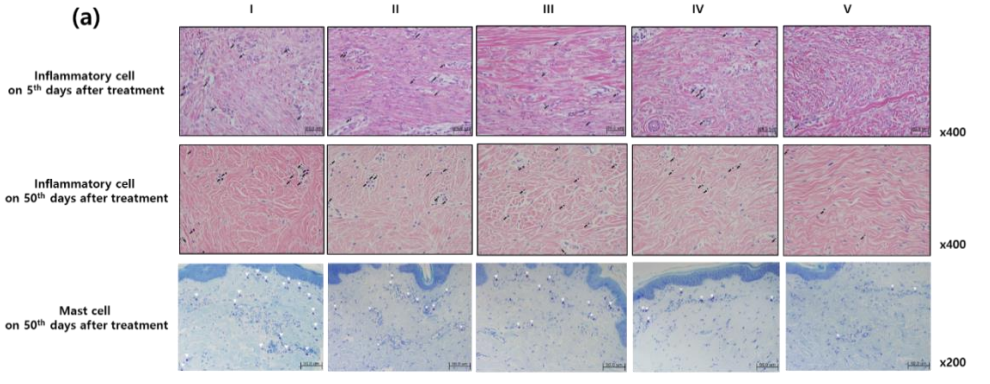

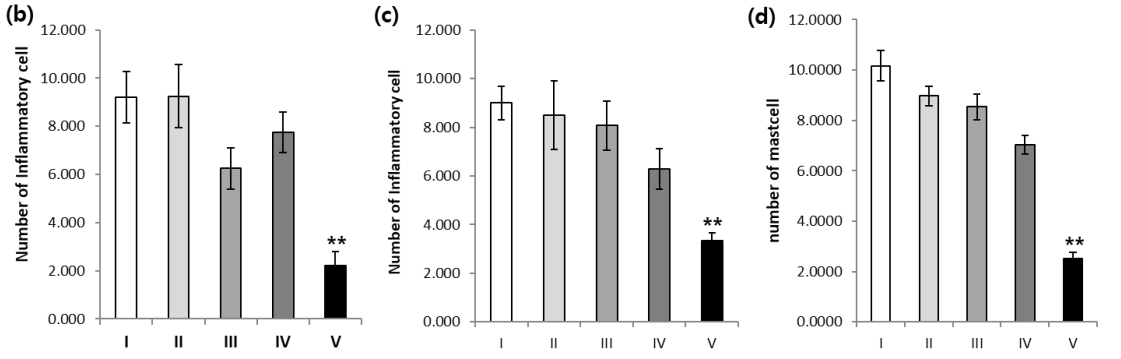

Figure 10. Inflammatory cell and mast cell count in pig scar tissue. (a) Inflammatory cell (black arrow) infiltration, as demonstrated by H&E staining (magnification, 400×) and mast cell (white arrow head) count with toluidine blue staining in the scar area. (b and c) The numbers of inflammatory cells on Days 5 and 50 were significantly lower in the alginate gel encapsulating dE1-k35/sLRP6E1E2-treated scar tissues (group V) (* $p < 0.05$). (d) The numbers of mast cells on Days 50 were significantly lower in the alginate gel encapsulating dE1-k35/sLRP6E1E2-treated scar tissues (group V) compared with other groups (* $p < 0.05$).

IV. DISCUSSION

Keloids are benign fibroproliferative scars that invade into surrounding normal skin beyond the original wound boundaries and keep growing slowly like a benign skin tumor[4]. The incidence has been reported about 16%[15], and they are highly associated with dark pigmented skin[16]. Unlike hypertrophic scars, they rarely regress spontaneously, resulting in both aesthetic problems and pain and functional disability.

Various mechanisms have been suggested to explain keloid pathogenesis; altered growth factor regulation, immune dysfunction, aberrant collagen turnover, sebum or sebocytes as self-antigens, altered mechanics, and altered apoptotic signaling in keloid fibroblasts[1,17]. Although a consistent theory is still lacking, TGF-β1 is known as a potent fibrogenic growth

factor that plays a primary role in keloid pathophysiology[2,18,19]. Thus, targeting TGF-β1 with pharmacologic interventions represents an attractive therapeutic option.

Skin injury involves response of Wnt/β-catenin pathway, with a critical role in epidermal stem cell maintenance, hair follicle development, regeneration and fibroblast-mediated scarring[20]. Activation of Wnt pathway plays a profibrotic role in cutaneous wound healing. Wnt/β-catenin signaling can upregulate TGF-β expression [21,22], and TGF-β1 can promote β-catenin signaling[23-25]. Furthermore, TGF-β stimulates canonical Wnt signaling by reducing the expression of the Wnt antagonist Dickkopf protein-1[26]. Prolonged activation of Wnt/β-catenin signaling has been observed in human hyperplastic wounds[27]. Therefore, inhibition of the canonical Wnt pathway might be an effective approach to target TGF-β signaling in fibrotic diseases such as keloids or hypertrophic scars.

We previously generated a novel soluble decoy Wnt receptor, sLRP6E1E2, which is composed of the low-density lipoprotein receptor-related protein 6 (LRP6) E1 and E2 regions, for functional interaction with Wnt and sLRP6E1E2-expressing replication-incompetent adenovirus (dE1-k35/sLRP6E1E2). An adenovirus in which both the E1 and E2 genes have been deleted blocks DNA replication and neosynthesis of viral protein. E1 encodes a transcription trans-activator crucial for the expression of genes key to viral replication, and E2 encodes a DNA-binding protein crucial for late gene transcriptional activation and viral replication[11]. As LRP6 plays a key role in activation of the canonical Wnt signaling pathway, these replication-defective Ad-based vectors engineered with the soluble decoy Wnt receptor sLRP6E1E2 induce an anti-fibrotic effect by inhibiting Wnt and TGF-β signaling. The effect was observed in vitro with human dermal fibroblasts and keloid spheroids in a previous study.

Using a pig scar model, we confirmed its therapeutic effect in vivo. Macroscopically, this approach helps to decrease scar size and minimize discoloration. Microscopically, we

observed that the collagen structure of scar tissue was become similar to normal tissue after treatment. Expression of structural proteins were decreased in treatment group. As in vitro results, sLRP6E1E2-expressing Ad downregulated TGF-β1 and upregulated TGF-β3 mRNA expression in vivo. In addition, expression of molecules that associated scar remodeling also convinced antifibrotic effect of sLRP6E1E2-expressing Ad. Expression level of MMP-1, which involves in the breakdown of extracellular matrix and tissue remodeling, breaking down the interstitial collagens, were increased in Ad-treated group. In contrast, TIMP-1, which has role in extracellular matrix remodeling by inhibitory activity of MMP-1[28,29], showed decreased expression level as well as α-SMA expression. The mast cells, known to be involved in the proliferation and contraction of fibroblasts, and the synthesis of ECM, which play a key role in scar formation, are also observed in fewer numbers in the virus-treated group. The numbers of inflammatory cells were lower in sLRP6E1E2-expressing Ad-treated group. Given that the keloid is the result of chronic inflammation of the reticula dermis[30], this result is also expected to provide a positive basis for treating problem scarring in the future.

Although adenovirus is an attractive gene delivery vector with the advantages of high gene-transfer ability, easy production/amplification, and low risk of insertional mutagenesis, its major drawback is rapid elimination of transduced cells[16]. As in vivo applications require long-term transduction, we introduced an Ad/alginate gel depot system. Previous studies indicated that the biological activity of Ad loaded in alginate gel is prolonged compared with that of naked Ad over an extended period of time[7]. And encapsulation of viral vectors may enhance therapeutic effect by masking viruses from clearance[9]. In this in vivo study, we confirmed that alginate gel-encapsulated decoy Wnt expressing Ad is more effective in scar management compared to naked Ad in a pig model. The alginate gel reservoir releases Ad in a sustained manner and maintains the biological activity of Ad longer. Alginate gel has also been shown to limit the Ad mobility by entrapping Ad within its scaffold, further minimizing

the spread of the replication-incompetent Ad outside the scar tissue. A microenvironment surrounded with alginate gel also protects the virus from clearance by the innate immune system.

V. CONCLUSION

Decoy Wnt receptor (sLRP6E1E2)-expressing adenovirus treatment improved scar quality in a pig model. Loading this construct in alginate gel allows sustained virus release into local tissues and prolongs Ad activity, thus maintaining its therapeutic effect longer in vivo. These advantages of the Ad/alginate system could markedly augment scar remodeling effects of sLRPE1E2 on scar tissue by steadily providing a high concentration of Ad with minimal toxicity.

References

1. Al-Attar A, Mess S, Thomassen JM, Kauffman CL, Davison SP. Keloid pathogenesis and treatment. Plast Reconstr Surg 2006;117:286-300.
2. Bran GM, Goessler UR, Hormann K, Riedel F, Sadick H. Keloids: current concepts of pathogenesis (review). Int J Mol Med 2009;24:283-93.
3. Tsai CH, Ogawa R. Keloid research: current status and future directions. Scars Burn Heal 2019;5:2059513119868659.
4. Burd A, Huang L. Hypertrophic response and keloid diathesis: two very different forms of scar. Plast Reconstr Surg 2005;116:150e-7e.
5. Atiyeh BS, Costagliola M, Hayek SN. Keloid or hypertrophic scar: the controversy: review of the literature. Ann Plast Surg 2005;54:676-80.
6. Lee WJ, Lee JS, Ahn HM, Na Y, Yang CE, Lee JH, et al. Decoy Wnt receptor (sLRP6E1E2)-expressing adenovirus induces anti-fibrotic effect via inhibition of Wnt and TGF-beta signaling. Sci Rep 2017;7:15070.
7. Choi JW, Kang E, Kwon OJ, Yun TJ, Park HK, Kim PH, et al. Local sustained delivery of oncolytic adenovirus with injectable alginate gel for cancer virotherapy. Gene Ther 2013;20:880-92.
8. Park H, Kim PH, Hwang T, Kwon OJ, Park TJ, Choi SW, et al. Fabrication of cross-linked alginate beads using electrospraying for adenovirus delivery. Int J Pharm 2012;427:417-25.
9. Koutsopoulos S, Unsworth LD, Nagai Y, Zhang S. Controlled release of functional proteins through designer self-assembling peptide nanofiber hydrogel scaffold. Proc Natl Acad Sci U S A 2009;106:4623-8.
10. Yun IS, Kang E, Ahn HM, Kim YO, Rah DK, Roh TS, et al. Effect of Relaxin Expression from an Alginate Gel-Encapsulated Adenovirus on Scar Remodeling in a Pig Model. Yonsei Med J 2019;60:854-63.

11. Lee JS, Hur MW, Lee SK, Choi WI, Kwon YG, Yun CO. A novel sLRP6E1E2 inhibits canonical Wnt signaling, epithelial-to-mesenchymal transition, and induces mitochondria-dependent apoptosis in lung cancer. PLoS One 2012;7:e36520.

12. Choi KJ, Zhang SN, Choi IK, Kim JS, Yun CO. Strengthening of antitumor immune memory and prevention of thymic atrophy mediated by adenovirus expressing IL-12 and GM-CSF. Gene Ther 2012;19:711-23.

13. Zhang SN, Choi IK, Huang JH, Yoo JY, Choi KJ, Yun CO. Optimizing DC vaccination by combination with oncolytic adenovirus coexpressing IL-12 and GM-CSF. Mol Ther 2011;19:1558-68.

14. Yun IS, Lee WJ, Rah DK, Kim YO, Park BY. Skin color analysis using a spectrophotometer in Asians. Skin Res Technol 2010;16:311-5.

15. Young WG, Worsham MJ, Joseph CL, Divine GW, Jones LR. Incidence of keloid and risk factors following head and neck surgery. JAMA Facial Plast Surg 2014;16:379-80.

16. Ud-Din S, Bayat A. New insights on keloids, hypertrophic scars, and striae. Dermatol Clin 2014;32:193-209.

17. Shih B, Garside E, McGrouther DA, Bayat A. Molecular dissection of abnormal wound healing processes resulting in keloid disease. Wound Repair Regen 2010;18:139-53.

18. Polakis P. Drugging Wnt signalling in cancer. Embo j 2012;31:2737-46.

19. Russell SB, Russell JD, Trupin KM, Gayden AE, Opalenik SR, Nanney LB, et al. Epigenetically altered wound healing in keloid fibroblasts. J Invest Dermatol 2010;130:2489-96.

20. Bastakoty D, Young PP. Wnt/beta-catenin pathway in tissue injury: roles in pathology and therapeutic opportunities for regeneration. Faseb j 2016;30:3271-84.

21. Lee WJ, Choi IK, Lee JH, Kim YO, Yun CO. A novel three-dimensional model system for keloid study: organotypic multicellular scar model. Wound Repair Regen 2013;21:155-65.

22. Carre AL, James AW, MacLeod L, Kong W, Kawai K, Longaker MT, et al. Interaction of wingless protein (Wnt), transforming growth factor-beta1, and hyaluronan production in fetal and postnatal fibroblasts. Plast Reconstr Surg 2010;125:74-88.

23. Sato M. Upregulation of the Wnt/beta-catenin pathway induced by transforming growth factor-beta in hypertrophic scars and keloids. Acta Derm Venereol 2006;86:300-7.

24. Guo Y, Xiao L, Sun L, Liu F. Wnt/beta-catenin signaling: a promising new target for fibrosis diseases. Physiol Res 2012;61:337-46.

25. Satterwhite DJ, Neufeld KL. TGF-beta targets the Wnt pathway components, APC and beta-catenin, as Mv1Lu cells undergo cell cycle arrest. Cell Cycle 2004;3:1069-73.

26. Logan CY, Nusse R. The Wnt signaling pathway in development and disease. Annu Rev Cell Dev Biol 2004;20:781-810.

27. Cheon S, Poon R, Yu C, Khoury M, Shenker R, Fish J, et al. Prolonged beta-catenin stabilization and tcf-dependent transcriptional activation in hyperplastic cutaneous wounds. Lab Invest 2005;85:416-25.

28. Ries C. Cytokine functions of TIMP-1. Cell Mol Life Sci 2014;71:659-72.

29. Jordan A, Roldan V, Garcia M, Monmeneu J, de Burgos FG, Lip GY, et al. Matrix metalloproteinase-1 and its inhibitor, TIMP-1, in systolic heart failure: relation to functional data and prognosis. J Intern Med 2007;262:385-92.

30. Ogawa R. Keloid and Hypertrophic Scars Are the Result of Chronic Inflammation in the Reticular Dermis. Int J Mol Sci 2017;18.

ABSTRACT (IN KOREAN)

돼지 모델을 이용한 알긴산염 겔에 쌓인 Decoy Wnt 수용체 발현 아데노바이러스의 흉터 리모델링 효과 연구

<지도교수 이원재>

연세대학교 대학원 의학과

최 세 운

Wnt decoy 수용체를 발현하는 아데노바이러스 벡터(Ad)는 Wnt 신호를 억제하면서 항섬유화 효과를 나타낸다고 알려져 있다. 우리는 이의 in vivo 효과를 돼지모델을 이용하여 확인하고, 알긴산염 겔 시스템을 이용하여 Ad 의 효과를 더 길게 유지해보고자 하였다.

먼저 여러 형태의 Ad 의 생물학적의 유전자 전달 효과를 형광 현미경을 이용하여 비교하였다. 그 다음은 요크셔 돼지의 등에 전층 피부 결손을 만들고 50 일 후에 다섯 그룹으로 나누어 치료를 진행하였다. (I, 대조군, II, 알긴산염, III, 알긴산염 겔로 쌓인 대조군, IV, naked LRP6, V, 알긴산염 겔에 쌓인 LRP6) 이들의 치료 효과를 확인하기 위하여 흉터의 사이즈와 멜라닌, 홍조 인덱스를 비교하였다. 또한 흉터 형성과 콜라겐섬유의 재배열에 영향을 줄 수 있는 여러 요소들을 조직학, 면역화학적, 면역

형광학적으로 분석하였다. 또한 세포외기질을 구성하는 주요 구성원에 대하여. RT-PCR 을 시행하고, 흉터 세포 내에 염증세포의 침윤 정도와 염증세포의 수를 계산하였다.

GFP 발현 정도를 비교한 결과 겔 안의 Ad 에서 더 강하고 긴 발현 정도를 나타내었다. 돼지 모델에서는 Ad 를 이용하여 치료한 그룹에서 흉터의 크기와 색소 측면에서 더 좋은 효과를 나타내었고, 특히 겔로 쌓인 Ad 로 치료한 그룹에서 통계적으로 유의한 효과를 나타내었다.

또한 조직 염색에서 그룹 V 의 조직은 미성숙한 콜라겐 침착이 유의하게 줄었고 콜라겐이 정상과 비슷하게 재배열 됨이 관찰되었다. 세포외기질의 주요 구성원인 1 형 콜라겐, 엘라스틴, 파이브로넥틴도 이 그룹에서 유의하게 감소하였다. 또한 해당 그룹에서 TGF-β1 mRNA 의 발현이 감소하고 TGF-β3 mRNA 의 발현이 증가하였으며 MMP-1 가 증가하고, TIMP, α-SMA 는 감소하였다. 염증세포 및 비만세포의 수도 감소하였다.

Ad 를 알긴산염 겔과 결합시키는 것은 이 바이러스를 조직에 천천히 방출하면서 그 효과를 오래 유지시키는 역할을 한다. 이를 이용하면 Ad 의 독성을 최소화하면서 조직에 이를 높은 농도로 지속적으로 제공하여 흉터 리모델링에 긍정적인 효과를 기대할 수 있다.

핵심되는 말 : 유전자치료, 아데노바이러스, Wnt, 흉터